IEEE Access
Multidisciplinary : Rapid Review : Open Access Journal

Received November 6, 2019, accepted December 1, 2019, date of publication December 13, 2019,
date of current version December 26, 2019.

Digital Object Identifier 10.1109/ACCESS.2019.2959427

Computational Fault Time Difference-Based Fault Location Method for Branched Power Distribution Networks

RUI CHEN[1], XIN YIN[2], (Member, IEEE), XIANGGEN YIN[1], (Member, IEEE), YILIN LI[1], AND JIAYUAN LIN[1]

[1]State Key Laboratory of Advanced Electromagnetic Engineering and Technology, Huazhong University of Science and Technology, Wuhan 430074, China
[2]Department of Electrical Engineering and Electronics, The University of Liverpool, Liverpool L693GJ, U.K.

Corresponding author: Xin Yin (xin.yin@liverpool.ac.uk)

This work was supported in part by the National Key Research and Development Program of China under Grant 2017YFB0902900 and Grant 2017YFB0902903.

ABSTRACT Fault location in a power distribution network is a challenging task due to the presence of multilayer branches and short line lengths. Existing fault-location methods generally require measurements at both ends of each branch, which requires a large number of measuring points. The placement of measuring points at branch terminals is an approach that can be used to reduce the number of measuring points. Such a measuring point layout allows the existing fault-location methods for power distribution networks to determine fault points after identifying faulted branches. However, these methods fail to locate a fault if the faulted branch cannot be correctly identified. This paper proposes a traveling-wave-based fault-location method for branched power distribution networks without requiring faulted branches to be identified. In the proposed method, by using the first arrival times of the fault-generated traveling waves detected at the substation and each branch terminal, the computational fault time difference (CFTD) is defined. By calculating the value of CFTD, the fault point is directly searched out. Finally, the quartile method is used to eliminate the impact of the arrival-time error on the fault-location accuracy of the proposed method. The simulation results verify the high accuracy, traveling-wave velocity stability, and strong arrival-time error robustness of the proposed method.

INDEX TERMS Power distribution network, fault location, traveling wave, computational fault time difference.

I. INTRODUCTION

Power distribution networks are connected to power consumers, and faults in a power distribution network directly cause power outages. Statistics show that the majority of customer interruptions originate at faults in power distribution networks. Accurate and reliable fault location is of great importance to reduce the system restoration time and the power outage time [1], [2].

The need for accurate and reliable fault location drives the evolution of fault-location algorithms. Among existing methods, those based on impedance [3]–[5] and traveling waves [6]–[10] are the most widespread. Impedance-based methods and some types of traveling-wave-based methods have been shown to work well for single-line power transmission networks [11]. For power distribution networks, existing methods perform poorly because of the presence of multilayer branches, the shortness of line lengths, and the lack of measuring points. The spread of wide-area measurement techniques and advanced measuring devices has started to overcome these limitations and can provide necessary measured data for fault location and decrease the investment cost of placing new metering points. Currently, several fault-location methods for power distribution networks have been reported. These methods generally require the placement of measuring points at substation and branch terminals. Such a measuring point layout allows these methods to determine fault points after identifying faulted branches. In [12], [13], impedance-based methods that utilize the measured data from substations and branch terminals are presented to identify faulted branches and determine fault points. In general, impedance-based methods require the voltages and the

The associate editor coordinating the review of this manuscript and approving it for publication was Taha Selim Ustun.

currents at the fault point and branch points/branch terminals to be estimated by using measured data and Kirchhoff's law. Therefore, the fault-location accuracies of these methods are affected by the measurement errors, line parameter errors, and equivalent load model accuracy. In addition, the difference between the estimated voltage at the fault point and the estimated voltages at branch points may small because of short line lengths. Therefore, impedance-based methods often perform poorly in practice. The method in [14] presents one way to locate a fault by comparing the precalculated arrival-time differences of the traveling waves with the measured time differences. Since the time differences corresponding to each point and each operation mode of the network need to be precalculated, the computational burden of this method is very large. In [15], a fault-location method based on the characteristic frequency of the traveling-wave propagation path is proposed. The characteristic frequency depends on the line parameters and the fault parameters. Since accurate parameters are difficult to obtain from the distribution networks, the accuracy of the method in [15] remains to be further discussed. The methods in [16], [17] identify the faulted branches by comparing the network parameters (that is, branch lengths) with a set of initial fault distances calculated by the classical two-terminal traveling-wave method; then, according to the results of faulted branch identification, the correct fault distances can be selected from the initial fault distances. However, these studies do not discuss the impact of the traveling-wave velocity on the fault-location accuracy. The method in [18] determines faulted branches and fault points by using a set of linear equations derived from the traveling-wave velocity and the first arrival times of the traveling waves detected at branch terminals. However, this method can precisely locate ground faults only if the traveling-wave velocity is highly accurate. In [19], a novel low-cost traveling-wave measuring device is applied to identify faulted branches and determine fault points. The method in [19] requires the devices to be accurately installed at the midpoint of each branch; otherwise, this method may have a large fault-location error. Furthermore, the impact of arrival-time errors is not considered in this method.

The above methods contribute to fault location in branched power distribution networks, but each method has unique disadvantages. In general, the identification of faulted branches is the main challenge. In fact, a minor measurement error or parameter error may cause the above methods to fail to correctly identify the faulted branch due to short line lengths and a lack of measuring points at branch points. In addition, although traveling-wave-based methods are sensitive to traveling-wave velocity inaccuracies and arrival-time error [20], traveling wave-based methods have shown higher accuracy and much stronger fault condition stabilization (time-varying load, distributed generation, system parameters, etc.) [6]–[10] than those of impedance-based methods. Therefore, traveling wave-based methods are more beneficial for fault location in distribution networks.

This paper proposes and validates a traveling-wave fault-location method for branched power distribution networks by utilizing the computational fault time difference (CFTD) derived from the first arrival times of the fault-generated traveling waves. Again, the identification of faulted branches in branched power distribution networks presents a major challenge for fault-location methods. Therefore, the value of the CFTD is used to directly search for fault points to overcome the need for faulted branch identification, which is the major contribution of this paper. Additionally, this paper takes into account that the traveling-wave velocity in power distribution networks is challenging to obtain accurately. Thus, the proposed method uses only the arrival time to derive the CFTD to overcome the impact of this inaccurate or unknown velocity on fault location. Moreover, the effect of arrival-time error on fault-location accuracy is considered, and the quartile method is used to eliminate this effect to improve fault-location accuracy. The proposed method is implemented by placing the measuring points at each branch terminal. A possible disadvantage of such a measuring point layout is the increasing cost of measuring devices as the number of terminals increases. However, the development and application of advanced measuring devices with low cost, such as that mentioned in [19], provide a way to overcome the abovementioned disadvantage.

II. BASIC CONCEPT AND CHARACTERISTICS OF THE CFTD

A. BASIC CONCEPT OF THE CFTD

The illustrative model is shown in Fig. 1. It is an overhead line network comprised of $n-2$ branches. The branches are connected to the main line at branch points b_1 to b_{n-2}. The traveling-wave detectors (TWDs) M_1 to M_n are placed at each branch terminal. Each TWD monitors the voltage and records the arrival time of the fault-generated traveling wave.

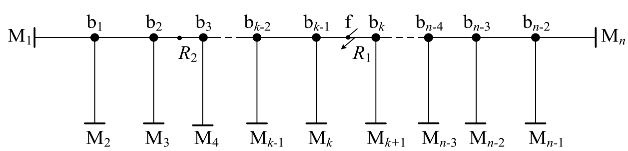

FIGURE 1. Diagram of an illustrative branched distribution network.

Assume that the fault occurs at f, the first arrival times of the traveling waves recorded by M_1 and M_j ($j \in [1, 2]$) are denoted by t_{M_1} and t_{M_j}. The reference points R_1 and R_2 are shown in Fig. 1. The computational fault time (CFT) for R_m ($m \in [1, 2]$) is defined as CFT_{R_m}. Regarding t_{M_1} as the reference time, CFT_{R_m} can be calculated by:

$$CFT_{R_m}(t_{M_1}, t_{M_j}) = t_{M_1} - \frac{l_{R_m M_1}}{l_{R_m M_1} - l_{R_m M_j}}(t_{M_1} - t_{M_j}) \quad (1)$$

where l_{fM_1} is the line length between f and M_1, l_{fM_j} is the line length between f and M_j, $l_{R_m M_1}$ is the line length between R_m and M_1, and $l_{R_m M_j}$ is the line length between R_m and M_j.

The difference between $CFT_{R_m}(t_{M_1}, t_{M_j})$ and $CFT_{R_m}(t_{M_1}, t_{M_p})$ ($p \neq j$) is defined as $\Delta CFT_{R_m.1_j-1_p}$. Furthermore, the CFTD for R_m is defined as $CFTD_{R_m}$. $\Delta CFT_{R_m.1_j-1_p}$ and $CFTD_{R_m}$ can be calculated by:

$$\Delta CFT_{R_m.1j-1p} = CFT_{R_m}(t_{\mathrm{M}_1}, t_{\mathrm{M}_j}) - CFT_{R_m}(t_{\mathrm{M}_1}, t_{\mathrm{M}_p}) \quad (2)$$

$$CFTD_{R_m} = \sqrt{\sum_{j=2}^{n-1} \sum_{p=j+1}^{n} \Delta CFT_{R_m.1j-1p}^2} \quad (3)$$

where $j \in [2, n-1]$ and $p \in [j+1, n]$. $CFTD_{R_m}$ consists of G items $\Delta CFT_{R_m.1_j-1_p}$, and G is given by:

$$G = \sum_{g=2}^{n-1} (n-g) \quad (4)$$

B. BASIC CHARACTERISTIC OF THE CFTD AT A FAULT POINT

Assume that the traveling-wave velocities between the fault point and the n TWDs are equal. According to the basic traveling-wave fault-location principle, the first arrival time of the fault-generated traveling waves can be described by:

$$\begin{cases} t_{\mathrm{M}_1} = \dfrac{1}{v} l_{\mathrm{fM}_1} + t_{\mathrm{f}} \\ t_{\mathrm{M}_j} = \dfrac{1}{v} l_{\mathrm{fM}_j} + t_{\mathrm{f}} \end{cases} \quad (5)$$

where t_{f} is the fault inception time, and v is the traveling-wave velocity.

Combining (1) and (5):

$$CFT_{R_m}(t_{\mathrm{M}_1}, t_{\mathrm{M}_j}) = t_{\mathrm{M}_1} - \frac{1}{v} \frac{l_{R_m\mathrm{M}_1}}{l_{R_m\mathrm{M}_1} - l_{R_m\mathrm{M}_j}} (l_{\mathrm{fM}_1} - l_{\mathrm{fM}_j}) \quad (6)$$

Assume that the reference point is located at the fault point f in Fig. 1, as shown by R_1. Taking into account $l_{\mathrm{fM}_1} = l_{R_1\mathrm{M}_1}$ and $l_{\mathrm{fM}_j} = l_{R_1\mathrm{M}_j}$, (6) can be rewritten as:

$$CFT_{R_1}(t_{\mathrm{M}_1}, t_{\mathrm{M}_j}) = t_{\mathrm{M}_1} - \frac{1}{v} l_{\mathrm{fM}_1} = t_{\mathrm{f}} \quad (7)$$

Furthermore, it can be easily obtained that:

$$\Delta CFT_{R_1.1j-1p} = 0 \quad (8)$$

$$CFTD_{R_1} = 0 \quad (9)$$

According to the above analysis, when the reference point is located at a fault point, the value of CFTD for this reference point is equal to zero.

C. BASIC CHARACTERISTIC OF THE CFTD AT A NON-FAULT POINT

As mentioned above, the value of CFTD for a fault point is equal to zero. Furthermore, if the value of CFTD for an arbitrary non-fault point is not equal to zero, then CFTD can be adapted to search for the fault point.

The CFTD for R_2 is used for analysis. According to (3), if each $\Delta CFT_{R_2.1_j-1_p}$ ($j \in [2, n-1]$, $p \in [j+1, n]$) is equal to zero, then $CFTD_{R_2}$ is equal to zero. Supposing an arbitrary $\Delta CFT_{R_2.1_j-1_p}$ is equal to zero, the following equation can be derived by combining (2) and (6).

$$\frac{1}{v} \frac{l_{R_2\mathrm{M}_1}}{l_{R_2\mathrm{M}_1} - l_{R_2\mathrm{M}_j}} (l_{\mathrm{fM}_1} - l_{\mathrm{fM}_j}) - \frac{1}{v} \frac{l_{R_2\mathrm{M}_1}}{l_{R_2\mathrm{M}_1} - l_{R_2\mathrm{M}_p}} (l_{\mathrm{fM}_1} - l_{\mathrm{fM}_p}) = 0 \quad (10)$$

Furthermore, l_{fM_1} can be solved with (10), that is:

$$l_{\mathrm{fM}_1} = \frac{l_{R_2\mathrm{M}_1} - l_{R_2\mathrm{M}_p}}{l_{R_2\mathrm{M}_j} - l_{R_2\mathrm{M}_p}} l_{\mathrm{fM}_j} - \frac{l_{R_2\mathrm{M}_1} - l_{R_2\mathrm{M}_j}}{l_{R_2\mathrm{M}_j} - l_{R_2\mathrm{M}_p}} l_{\mathrm{fM}_p} \quad (11)$$

Taking into account $l_{\mathrm{fM}_1} \geq 0$, (11) can be rewritten as:

$$\frac{l_{R_2\mathrm{M}_1} - l_{R_2\mathrm{M}_p}}{l_{R_2\mathrm{M}_1} - l_{R_2\mathrm{M}_j}} \geq \frac{l_{\mathrm{fM}_p}}{l_{\mathrm{fM}_j}} \quad (12)$$

Similarly, taking into account $l_{\mathrm{fM}_j} \geq 0$ and$l_{\mathrm{fM}_p} \geq 0$, (13) or (14) can be easily derived from (12):

$$\begin{cases} l_{R_2\mathrm{M}_1} \geq l_{R_2\mathrm{M}_j} \\ l_{R_2\mathrm{M}_1} \geq l_{R_2\mathrm{M}_p} \end{cases} \quad (13)$$

$$\begin{cases} l_{R_2\mathrm{M}_1} \leq l_{R_2\mathrm{M}_j} \\ l_{R_2\mathrm{M}_1} \leq l_{R_2\mathrm{M}_p} \end{cases} \quad (14)$$

Equation (13) and (14) can be considered as the preconditions that an arbitrary $\Delta CFT_{R_2.1_j-1_p}$ is equal to zero, and these two preconditions cannot be met simultaneously.

Furthermore, if each $\Delta CFT_{R_2.1_j-1_p}$ is equal to zero (i.e., $CFTD_{R_2}$ is equal to zero), then the corresponding precondition can be derived: $l_{R_2\mathrm{M}_1} \geq l_{R_2\mathrm{M}_x}$ or $l_{R_2\mathrm{M}_1} \leq l_{R_2\mathrm{M}_x}$ ($x \in [2, n-1]$). If this precondition is met, then $CFTD_{R_2}$ may be equal to zero. However, in practice, this precondition presents a highly unlikely scenario due to the complex structure of power distribution networks. Thus, it can be concluded that the value of $CFTD_{R_2}$ can be always considered to be nonzero. This conclusion is valid for the CFTD for an arbitrary non-fault point.

III. PROPOSED FAULT LOCATION METHOD

A. PHASE-MODEL TRANSFORMATION

Since traveling waves are mutually coupled in a three-phase power system, the phase domain signals are generally decomposed into the modal domain components (aerial modal and ground modal). The aerial modal traveling wave is much more stable than the ground modal wave because its dispersion is not obvious. Further, for a power distribution network with a single type of distribution line (overhead line or cable), the velocity of the aerial modal traveling wave can be regarded as a constant [14]–[19]. Thus, in this paper, the measured voltages are converted to their modal components by means of the Clarke transformation [21], and the aerial modal component (modal 1) is used for fault location.

B. DETECTION OF THE FIRST ARRIVAL TIME OF THE FAULT-GENERATED TRAVELING WAVES

In this subsection, the first arrival times of the fault-generated traveling waves are detected. Several methods for this step are available in the literature, such as the S transform method [16], [22], [23], the wavelet transform method [24], and the Park transformation [25]. Notably, the aim of this paper is to demonstrate the performance and advantages of the proposed fault location method, not to evaluate the performance of traveling wave detection methods. In this paper, the S transform is used to detect the first arrival times of the aerial modal traveling waves since it has the advantages of both multiresolution analysis and single-frequency analysis [16], [22], [23].

The S transform is a classical signal processing method, and its basic principle has been detailed in [16], [22], [23] and is not repeated here. In this paper, only the S transform-based detection method for the first arrival times is described. The output of the S transform is a complex matrix usually known as the S matrix, whose columns pertain to time and rows pertain to frequency. Furthermore, the detection method can be described as follows [22]: calculate the modulus of each element within the row vector corresponding to the frequency f_S; the sampling time corresponding to the maximum modulus is the first arrival time of the traveling wave. In general, the arbitrary frequency contained in traveling waves can be set to f_S.

C. SEARCH OF THE FAULT POINT

In this subsection, a CFTD-based fault-location method is presented. Assume that a fault occurs at an arbitrary position in a power distribution network with N terminals, N TWDs (one per terminal), and X reference points. Next, assume that the first arrival times of the fault-generated traveling waves recorded by the TWDs are denoted by t_{M_1} to t_{M_N}. Regarding t_{M_i} ($i \in N$) as the reference time, (1), (2), and (3) are rewritten as (15), (16), and (17), respectively:

$$CFT_{R_m}(t_{M_i}, t_{M_j}) = t_{M_i} - \frac{l_{R_m M_i}}{l_{R_m M_i} - l_{R_m M_j}}(t_{M_i} - t_{M_j}) \tag{15}$$

$$\Delta CFT_{R_m.ij-ip} = CFT_{R_m}(t_{M_i}, t_{M_j}) - CFT_{R_m}(t_{M_i}, t_{M_p}) \tag{16}$$

where $j \in [2, N-1]$ and $p \in [j+1, N]$.

$$CFTD_{R_m.i} = \sqrt{\sum_{\substack{j=1 \\ j\neq i}}^{N-1} \sum_{\substack{p=j+1 \\ p\neq i}}^{N} (\Delta CFT_{R_m.ij-ip})^2} \tag{17}$$

where $CFTD_{R_m.i}$ is the CFTD for R_m with reference time $t_{M\,i}$. Similarly, $CFTD_{R_m.i}$ comprises G items.

CFTD for reference point R_m ($m \in X$) can be calculated, and an array $\boldsymbol{CFTD}_i = \{CFTD_{R_1.i} \ldots CFTD_{R_m.i} \ldots CFTD_{R_X.i}\}$ can be obtained. According to the analysis in Section II, the value of CFTD for the fault point is theoretically equal to zero. However, in practice, the CFTD would be a very small value due to the impact of arrival-time errors and calculation errors. Therefore, the reference point corresponding to the minimum in $\boldsymbol{CFTD}_i$ is considered the fault point, and this reference point is denoted by R_{fault}.

Then, an arbitrary TWD is set as the reference TWD, denoted by M*. The fault distance $l_{\mathrm{fM}^*.i}$ between R_{fault} and M* can be obtained:

$$l_{\mathrm{fM}^*.i} = l_{R_{\mathrm{fault}}\mathrm{M}^*.i} \tag{18}$$

where the subscript i is the serial number of reference time.

By regarding each arrival time as the reference time, N fault distances can be calculated, and the fault distance array $\boldsymbol{L} = \{l_{\mathrm{fM}^*.1} \ldots l_{\mathrm{fM}^*.i} \ldots l_{\mathrm{fM}^*.N}\}$ can be obtained. An analysis of (15), (16), (17), and (18) indicates that the accuracies of the fault distances in $\boldsymbol{L}$ are dependent on how accurately the arrival times are recorded. If the arrival times are highly accurate, then the fault distances in $\boldsymbol{L}$ are equal, and each fault distance presents the actual fault distance with a high accuracy. If the arrival times are inaccurate, the arrival-time errors result in decreases in the accuracies of the fault distances in $\boldsymbol{L}$. The fault distances with lower accuracy can be considered "bad" data. In this paper, the quartile method is used to eliminate the bad data in $\boldsymbol{L}$ to improve the fault-location accuracy; this process is described in the next subsection. Then, the average value of the normal data in $\boldsymbol{L}$ is the final fault distance.

D. ELIMINATION OF THE ABNORMAL DATA

In this subsection, the quartile method [26] is used to eliminate the bad data in $\boldsymbol{L}$. According to [26], the interquartile range of $\boldsymbol{L}$ is given by:

$$I_{QR} = Q_3 - Q_1 \tag{19}$$

where I_{QR} is the interquartile range of $\boldsymbol{L}$ and Q_1 and Q_3 are the first quartile and the third quartile, respectively. The method for computing Q_1 and Q_3 is given in [26].

Furthermore, $l_{\mathrm{fM}^*.i}$ ($i \in N$) outside the boundary shown in (20) can be considered as the data. Then, the average value of the normal data in $\boldsymbol{L}$, that is, the final fault distance, can be calculated.

$$[F_{\min}, F_{\max}] = [Q_1 - 1.5I_{QR}, Q_3 + 1.5I_{QR}] \tag{20}$$

E. ADAPTATION OF THE PROPOSED METHOD FOR OVERHEAD LINE-CABLE HYBRID DISTRIBUTION NETWORKS

According to (15), (16), and (17), the CFTD is independent of the traveling-wave velocity. Thus, the proposed method has an advantage that the fault-location accuracy does not affect by the traveling-wave velocity. However, this advantage requires the invariable traveling-wave velocity. For an overhead line power distribution network or a cable distribution network, the dispersion of the aerial modal traveling waves is stable, and the velocity of the aerial modal traveling wave can be regard as a constant. For an overhead line-cable hybrid power distribution network, the traveling-wave dispersion in the overhead line and the cable are significantly different due to the differences in the structure and the conductor size. Thus, the traveling-wave velocity in overhead lines is different from the velocity in the cables. This velocity difference decreases the fault-location accuracy of the proposed method. Converting a cable into an equivalent overhead line is a way to overcome the impact of this velocity difference. The length of the equivalent overhead line can be calculated by (21) [27]:

$$l_{eq} = \frac{v_{overhead}}{v_{cable}} l_{cable} \tag{21}$$

where l_{eq} is the length of the equivalent overhead line, l_{cable} is the actual length of a cable, $v_{overhead}$ is the traveling-wave velocity in overhead line, and v_{cable} is the traveling-wave velocity in cable. $v_{overhead}$ and v_{cable} can be calculated by using the parameters of the distribution lines [19].

After converting all cables into the equivalent overhead lines, the hybrid power distribution network is converted into an equivalent network consisting of the original overhead lines and the equivalent overhead lines. In this equivalent network, the velocity difference between overhead lines and cables is eliminated, and the traveling-wave velocity in this equivalent network can be regarded as a constant. Then, the fault point and the fault distance can be determined by using the CFTD-based fault-location method introduced in section III C and D. In addition, if the fault path corresponding to the fault distance contains the equivalent overhead lines, this fault distance should be converted again to obtain a more accurate fault distance:

$$l^* = (l' - l_{overhead})\frac{v_{cable}}{v_{overhead}} + l_{overhead} \tag{22}$$

where l^* is the actual fault distance, l' is the equivalent fault distance (i.e., the fault distance calculated in the equivalent network), and $l_{overhead}$ is the length of the overhead lines in l'.

Furthermore, (21) and (22) require the parameters of the distribution lines to calculate $v_{overhead}$ and v_{cable}. However, parameters of the distribution lines are difficult to obtain from the distribution networks. Thus, in this paper, the experiential values of $v_{overhead}$ and v_{cable} are used for the conversion. In general, the experiential velocities for the overhead lines and cables are equal to 98% and 57%–65% of the speed of light, respectively [20]. Notably, the use of the experiential traveling-wave velocities results in a conversion error, and this conversion error may cause a fault-location error. However, the proposed method can overcome the effect of this conversion error because the redundant arrival times are used to calculate the CFTD.

F. THE FLOWCHART AND CHARACTERISTICS OF THE PROPOSED FAULT-LOCATION METHOD

The flowchart of the proposed fault-location method is shown in Fig. 2. For a real power distribution system, the proposed method can be implemented by placing measuring devices at each branch terminal. Furthermore, the measuring devices required by the proposed method should be able to detect the fault-generated traveling wave and should be equipped with a global positioning system (GPS) and a communication link. In addition, the distance between the two adjacent reference points should be less than twice the length of the required fault-location accuracy and able to be flexibly adjusted according to the scale of the power distribution network. Considering the impact of the errors (measurement error, calculation error, conversion error, etc.) on the fault-location accuracy, a margin for the distance step should also be considered. In practice, variable distance steps can be used to enhance the practicability of our proposed method: the CFTD is calculated by a large distance step, and the initial fault point can be determined; then a smaller distance step is used to calculate the CFTD to determine the accurate fault point.

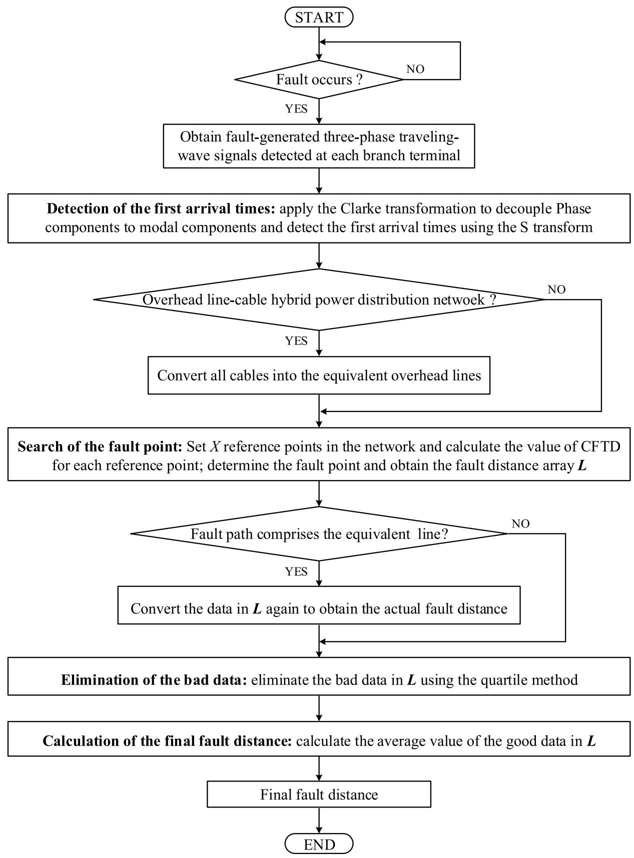

FIGURE 2. Flowchart of the proposed fault-location method.

According to (15), (16), (17), (18), and the aforementioned analysis, the following characteristics of the proposed fault-location method can be obtained:

1) The proposed method selects the fault point from the reference points. Therefore, the proposed method does not require the identification of the faulted branch.
2) The arrival times for calculating CFTD are highly redundant. Meanwhile, the bad data (i.e., the fault distances that are seriously affected by the arrival-time errors) in fault distance array $\boldsymbol{L}$ are eliminated by the quartile method. Thus, the proposed method is robust to arrival-time errors.
3) For a power distribution network with a single type of distribution line (overhead line or cable), the CFTD is independent of the traveling-wave velocity. For

an overhead line-cable hybrid power distribution network, the conversion error caused by the experiential traveling-wave velocities may affect the accuracy of the CFTD. However, the effect of the conversion error can be overcome because redundant data are used to calculate the CFTD. Thus, the proposed method presents a stability to the traveling-wave velocity.

IV. PERFORMANCE EVALUATION

A. SIMULATION MODEL

The example network in this paper, shown in Fig. 3, is based on the United Kingdom Generic Distribution System (UKGDS)'s 'Rural' network (11kV) [18]. In total, 15 TWDs are placed at the branch terminals and labeled M_1 to M_{15}. M_1 is selected as the reference TWD, that is, M^*. For clarity, the branch points are labeled b_1 to b_{12}. The distribution lines in Fig. 3 are all overhead lines, and their lengths are shown in Fig. 3. The additional network data can be obtained from [28]. The simulation of the example network is carried out using PSCAD. The PSCAD-generated simulation data are then imported into MATLAB, where the proposed algorithm is implemented. In all simulations, frequency-dependent Marti line models [29] are used to implement the overhead lines, and a sampling frequency of 10 MHz is used. For convenience, an identical configuration is assumed for each overhead line. The distance between adjacent reference points is 20 m; a summary of the position of the reference points is shown in TABLE 1. In all the simulations, the Clarke transformation is used to transform the voltage signals from the phase domain into the modal domain; then, the S transform is performed on aerial modal (modal 1) voltages. f_S is chosen to be the Nyquist frequency.

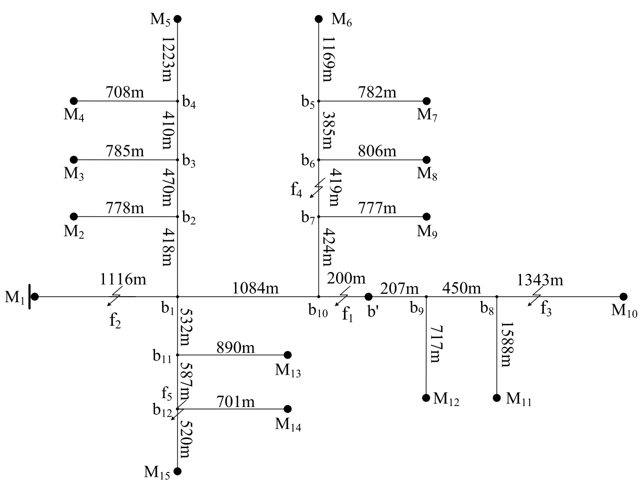

FIGURE 3. Example network.

To evaluate the performance of the proposed method, the percent error for fault location is used:

$$error\ \% = \left| \frac{l_{fM^*.actual} - l_{fM^*.calculated}}{l_{total}} \right| \times 100 \tag{23}$$

where $l_{fM^*actual}$ is the actual fault distance, $l_{fM^*.calculated}$ is the calculated fault distance, and l_{total} is the total branch length.

TABLE 1. Position of the reference points.

Reference point	Start	End	Reference point	Start	End
R_1-R_{218}	M_1	M_{10}	R_{609}-R_{647}	b_6	M_8
R_{219}-R_{342}	b_1	M_5	R_{648}-R_{685}	b_7	M_9
R_{343}-R_{380}	b_2	M_2	R_{686}-R_{763}	b_8	M_{11}
R_{381}-R_{418}	b_3	M_3	R_{764}-R_{798}	b_9	M_{12}
R_{419}-R_{452}	b_4	M_4	R_{799}-R_{879}	b_1	M_{15}
R_{453}-R_{570}	b_{10}	M_6	R_{880}-R_{922}	b_{11}	M_{13}
R_{571}-R_{608}	b_5	M_7	R_{923}-R_{956}	b_{12}	M_{14}
R_{571}-R_{608}	b_5	M_7	R_{923}-R_{956}	b_{12}	M_{14}

B. PERFORMANCE OF THE PROPOSED METHOD

Assume that a single-line-to-ground fault (A-g) with a fault resistance of 50 Ω and a fault angle of 60° occurs at f_1 (i.e., R_{115}), 2300 m from M^*. The fault inception time is set to 0.1033 s. The results of S transform and the first arrival times of the traveling waves are shown in Fig. 4 and TABLE 2.

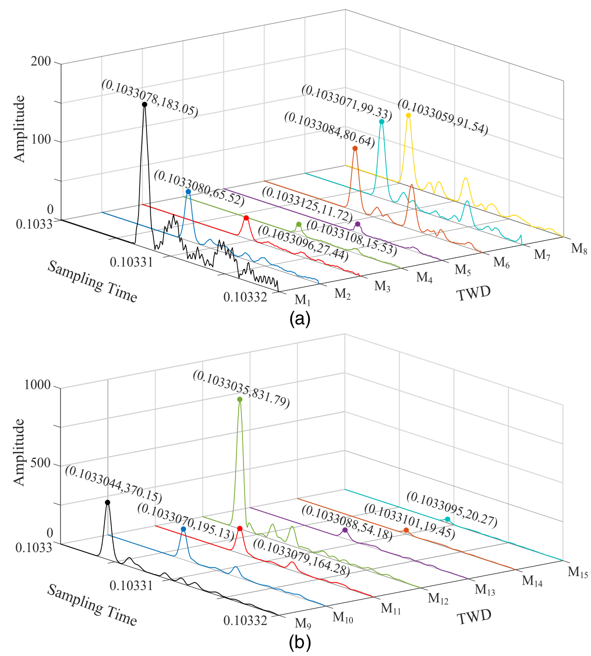

FIGURE 4. The first arrival times of the traveling-waves. (a) arrival times detected at M_1 to M_8; (b) arrival times detected at M_9 to M_{15}.

TABLE 2. Arrival times for the fault at f_1.

TWD	Arrival time	TWD	Arrival time	TWD	Arrival time
M_1	0.1033078	M_6	0.1033084	M_{11}	0.1033079
M_2	0.1033080	M_7	0.1033071	M_{12}	0.1033035
M_3	0.1033096	M_8	0.1033059	M_{13}	0.1033088
M_4	0.1033108	M_9	0.1033044	M_{14}	0.1033101
M_5	0.1033125	M_{10}	0.1033070	M_{15}	0.1033095

The results of $\boldsymbol{CFTD_i}$ ($i \in [1, 15]$) are shown in Fig. 5. This figure illustrates that the value of CFTD is minimized at the fault position regardless of which arrival time is regarded as the reference time. The minimum of $\boldsymbol{CFTD_i}$ is listed in TABLE 3. The fault point (i.e., $R_{\text{fault}.i}$) and fault distance (i.e., $l_{\text{fM}^*.i}$) are also listed in TABLE 3.

$\boldsymbol{L}$ can be obtained from the data in TABLE 3:

$$\boldsymbol{L} = \{2300\ \ 2300\ \ 2300\ \ 2280\ \ 2300\ \ 2300\ \ 2300\ \ 2320\ \ 2300\ \ 2320\ \ 2300\ \ 2300\ \ 2300\ \ 2300\}$$

$F_{\min}$ and $F_{\max}$ of $\boldsymbol{L}$ can be calculated through (20) and are both 2300. Thus, there are no bad data in $\boldsymbol{L}$. The final fault distance is 2301.33 m (i.e., the average value of the good data in $\boldsymbol{L}$), the corresponding percent error of fault-location is 0.0067%.

TABLE 3. Results of the minimum *CFTD*, fault point, and fault distance for the fault at f_1.

Serial Number	Reference Time	Minimum of $\boldsymbol{CFTD_i}$	$R_{\text{fault}.i}$	$l_{\text{fM}^*.i}$ (m)
1	t_{M_1}	19.9385	R_{115}	2300
2	t_{M_2}	19.6385	R_{115}	2300
3	t_{M_3}	19.0473	R_{115}	2300
4	t_{M_4}	18.6348	R_{114}	2280
5	t_{M_5}	17.4811	R_{115}	2300
6	t_{M_6}	18.7573	R_{115}	2300
7	t_{M_7}	20.3810	R_{115}	2300
8	t_{M_8}	18.2356	R_{116}	2320
9	t_{M_9}	17.7408	R_{115}	2300
10	$t_{M_{10}}$	20.3844	R_{115}	2300
11	$t_{M_{11}}$	19.7941	R_{116}	2320
12	$t_{M_{12}}$	17.5869	R_{115}	2300
13	$t_{M_{13}}$	18.8376	R_{115}	2300
14	$t_{M_{14}}$	18.6806	R_{115}	2300
15	$t_{M_{15}}$	18.9907	R_{115}	2300

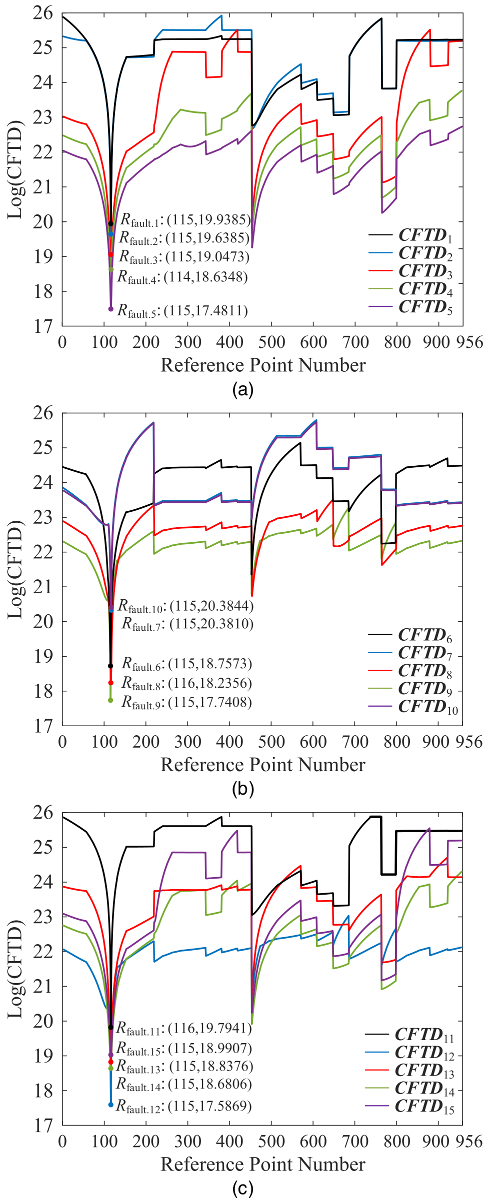

FIGURE 5. The value of *CFTD*. (a) $\boldsymbol{CFTD_1}$ to $\boldsymbol{CFTD_5}$; (b) $\boldsymbol{CFTD_6}$ to $\boldsymbol{CFTD_{10}}$; (c) $\boldsymbol{CFTD_{11}}$ to $\boldsymbol{CFTD_{15}}$.

C. PERFORMANCE OF THE PROPOSED METHOD CONSIDERING ARRIVAL TIME ERROR

The accuracy of the proposed method depends on how accurately the arrival time can be recorded. Therefore, two situations are considered: 1) a single arrival time with a large individual error; and 2) all arrival times have errors, which are all different. In both situations, the aforementioned fault at f_1 is used for analysis.

1) SIMULATION WITH A LARGE INDIVIDUAL ERROR

Assume that an error of 20 μs is imposed on t_{M_1}, and no error is imposed on the other arrival times. The simulation results are listed in TABLE 4.

From TABLE 4, the corresponding $\boldsymbol{L}$ can be obtained:

$$\boldsymbol{L} = \{1700\ \ 2300\ \ 2280\ \ 2160\ \ 2100\ \ 2300\ \ 2300\ \ 2320\ \ 2300\ \ 2300\ \ 2320\ \ 2380\ \ 2380\ \ 2360\ \ 2380\}$$

$F_{\min}$ and $F_{\max}$ of $\boldsymbol{L}$ can be calculated, those are 2212 and 2352, respectively. Then, the bad data can be obtained and are 1700, 2100, and 2160. Furthermore, the final fault distance is 2291.66 m, and the percent error of fault-location is 0.0426%.

Notably, in TABLE 4, the fault distances derived by $\boldsymbol{CFTD}_2$ to $\boldsymbol{CFTD}_{15}$ are much more accurate than the distance derived by the $\boldsymbol{CFTD}_1$. To demonstrate the differences in accuracy, $\boldsymbol{CFTD}_1$ and $\boldsymbol{CFTD}_2$, shown in Fig. 6, are used for analysis. It is observed that, in general, individual arrival time error leads to a decrease in the value of the CFTD across all reference points. However, this effect depends on which arrival time has an error and the selection of the reference time. Furthermore, in this situation, $\boldsymbol{CFTD}_1$ and $\boldsymbol{CFTD}_2$ comprise 956 $CFTD_{R_m.1}$ items and 956 $CFTD_{R_m.2}$ items ($m \in [1, 956]$), respectively. According to (15), (16), and (17), both $CFTD_{R_m.1}$ and $CFTD_{R_{m}.2}$ comprise G items.

TABLE 4. Results for a simulation with a large individual error.

Serial Number	Reference Time	Minimum of $\boldsymbol{CFTD_i}$	R_{fault}	$l_{\text{fM*}.i}$ (m)
1	t_{M_1}	19.6122	R_{85}	1700
2	t_{M_2}	19.6007	R_{115}	2300
3	t_{M_3}	18.9055	R_{114}	2280
4	t_{M_4}	17.9183	R_{108}	2160
5	t_{M_5}	17.0301	R_{105}	2100
6	t_{M_6}	27.8208	R_{115}	2300
7	t_{M_7}	19.9159	R_{115}	2300
8	t_{M_8}	17.7102	R_{116}	2320
9	t_{M_9}	17.1072	R_{115}	2300
10	$t_{\text{M}_{10}}$	19.9023	R_{115}	2300
11	$t_{\text{M}_{11}}$	18.8270	R_{115}	2300
12	$t_{\text{M}_{12}}$	17.0087	R_{114}	2280
13	$t_{\text{M}_{13}}$	17.8429	R_{114}	2280
14	$t_{\text{M}_{14}}$	18.0808	R_{113}	2260
15	$t_{\text{M}_{15}}$	17.8979	R_{114}	2280

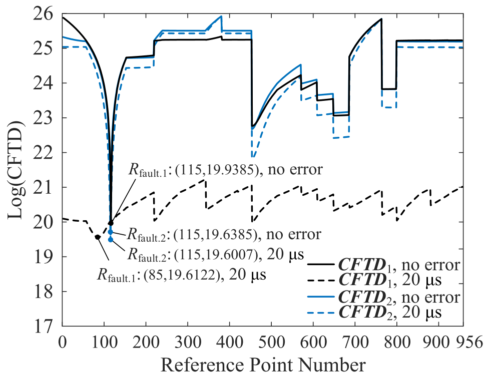

FIGURE 6. Effect of a large timestamp error.

Each item of $CFTD_{R_m.1}$ includes $t_{\text{M}1}$ and is affected by the arrival time error. Meanwhile, only 13 items of $CFTD_{R_{\text{m}.2}}$ include $t_{\text{M}1}$ and are affected by the arrival time error. For this reason, the decrease in $CFTD_{R_m.1}$ is much more obvious than the decrease in $CFTD_{R_{\text{m}.2}}$, and the fault distance derived by $\boldsymbol{CFTD}_1$ is more sensitive to arrival time error. To improve the fault location accuracy, the fault distances derived by $\boldsymbol{CFTD}_1$ should be eliminated. This is the reason that the quartile method is used in this paper.

In this situation, if the bad data in $\boldsymbol{L}$ are not eliminated, then the final fault distance and the corresponding error are 2230.7 m and 0.3555%, respectively. According to the aforementioned calculation results, the error is reduced from 0.3555% to 0.0426% after eliminating the bad data, and the fault-location accuracy is increased by 70%.

2) SIMULATION WITH NONIDENTICAL ARRIVAL TIME ERRORS

Assume that the error values of -1 μs to 1 μs are randomly added to each arrival time. In this situation, five cases are simulated, as shown in TABLE 5. The fault-location percent errors of the proposed method are shown in Fig. 7. To better illustrate the performance of the proposed method, the percent errors of the proposed method are compared with the errors of the existing fault-location method as shown in Fig. 7.

TABLE 5. Arrival time errors for each case considered.

Arrival Time	Timestamp error (µs) Case 1	Case 2	Case 3	Case 4	Case 5
t_{M_1}	+0.5	+0.6	−0.5	−0.7	+0.1
t_{M_2}	+0.8	+0.4	−0.3	+0.7	−0.3
t_{M_3}	−0.1	−0.3	+0.4	+0.2	−0.8
t_{M_4}	−0.6	−0.2	+0.3	+0.6	+0.7
t_{M_5}	+0.2	+0.3	−0.4	−0.3	−0.5
t_{M_6}	+0.1	+0.8	−0.9	+0.2	−0.4
t_{M_7}	−1.0	−0.5	+0.4	+0.4	+0.3
t_{M_8}	+1.0	+0.6	−0.7	−0.6	−0.6
t_{M_9}	+0.4	+0.7	−0.6	−0.3	+1.0
$t_{\text{M}_{10}}$	+0.3	+0.6	−0.5	+1.0	−1.0
$t_{\text{M}_{11}}$	+0.6	+0.2	−0.3	−0.4	+0.3
$t_{\text{M}_{12}}$	+0.8	+0.1	−0.2	+0.6	−0.6
$t_{\text{M}_{13}}$	−0.5	−0.8	+0.9	−1.0	+0.8
$t_{\text{M}_{14}}$	−0.9	−0.4	+0.5	+0.2	−0.7
$t_{\text{M}_{15}}$	−0.4	−0.6	+0.7	−0.3	+0.2

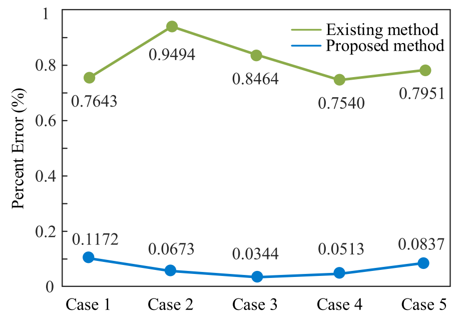

FIGURE 7. Error of fault location considering the various arrival time errors.

The existing method estimates a set of initial fault distances by using the classical two-terminal traveling-wave method [18], [27], and the weighted average value of these initial fault distances is the final fault distance. In general, if the initial distance is less than zero, then its weight is zero; if the initial distance is greater than zero, then the average weight is used. For the existing method, the faulted branch is assumed to be known.

It can be seen that the maximum and average percent errors of the proposed method are 0.1172% and 0.0708%, and the corresponding maximum and average absolute errors are 22.85 m and 13.80 m. Meanwhile, the maximum and average percent errors of the existing method are 0.9490% and 0.8218%, that is, 185.01 m and 160.21 m. Compared with the existing method, the maximum percent error of the proposed method decreases by 0.8318% (i.e., 162.16 m) and the average percent is decreases by 0.751% (i.e., 146.41 m). The above results show that the fault-location accuracy of the proposed method is higher than that of the existing method because of the strong arrival-time error robustness of the proposed method.

D. PERFORMANCE OF THE PROPOSED METHOD IN THE OVERHEADLINE-CABLE HYBRID NETWORK

To illustrate the performance of the proposed method in the overhead-line-cable hybrid power distribution network, the line b_{10}-b' (i.e., the line between b_{10} and b′) in Fig. 3 is modified from the overhead line to the cable. The velocities of the aerial modal traveling wave in the overhead line and cable calculated by the line parameters are 2.942×10^5 km/s and 1.7052×10^5 km/s, respectively. The aforementioned fault at f_1 is used for the analysis. The first arrival times of the traveling waves are shown in TABLE 6.

TABLE 6. The first arrival times considering the hybrid line.

TWD	Arrival time	TWD	Arrival time	TWD	Arrival time
M_1	0.1033085	M_6	0.1033092	M_{11}	0.1033084
M_2	0.1033087	M_7	0.1033079	M_{12}	0.1033043
M_3	0.1033104	M_8	0.1033064	M_{13}	0.1033096
M_4	0.1033117	M_9	0.1033052	M_{14}	0.1033107
M_5	0.1033134	M_{10}	0.1033077	M_{15}	0.1033101

Since accurate line parameters are difficult to obtain in practice, a 5% conversion error is considered. Then, the cable between b_{10} and b’ is converted into an equivalent overhead by using (21), and its equivalent length is 344.83 m. The simulation results are listed in TABLE 7.

TABLE 7. Results of the simulation considering the hybrid line.

Serial Number	Reference Time	Minimum of $\boldsymbol{CFTD_i}$	R_{fault}	$l_{fM^*.i}$ (m)
1	t_{M_1}	20.2831	R_{120}	2400
2	t_{M_2}	20.0189	R_{120}	2400
3	t_{M_3}	20.7404	R_{120}	2400
4	t_{M_4}	19.8065	R_{118}	2360
5	t_{M_5}	18.8403	R_{119}	2380
6	t_{M_6}	19.8987	R_{120}	2400
7	t_{M_7}	19.7704	R_{120}	2400
8	t_{M_8}	19.9123	R_{118}	2360
9	t_{M_9}	19.4490	R_{119}	2380
10	$t_{M_{10}}$	19.7972	R_{120}	2400
11	$t_{M_{11}}$	20.2867	R_{120}	2400
12	$t_{M_{12}}$	19.0607	R_{118}	2360
13	$t_{M_{13}}$	20.2527	R_{121}	2420
14	$t_{M_{14}}$	20.5819	R_{120}	2400
15	$t_{M_{15}}$	20.6732	R_{119}	2380

It can be seen that the fault path corresponding to each fault distance $l_{fM^*.i}$ in TABLE 7 contains the equivalent overhead line. Thus, $l_{fM^*.i}$ should be converted again to obtain more accurate fault distances by using (22). The conversion results are shown in TABLE 8.

From TABLE 8, the corresponding $\boldsymbol{L}$ can be obtained:

$$\boldsymbol{L} = \{2318.52\ \ 2318.52\ \ 2318.52\ \ 2295.32\ \ 2306.92\ \ 2318.52\ \ 2318.52\ \ 2295.32\ \ 2306.92\ \ 2318.52\ \ 2318.52\ \ 2295.32\ \ 2330.12\ \ 2318.52\ \ 2306.92\}$$

$F_{\min}$ and $F_{\max}$ of $\boldsymbol{L}$ can be calculated, those are 2289.52 and 2335.92, respectively. Thus, there is no bad data in $\boldsymbol{L}$. The final fault distance is 2309.93 m, the corresponding percent error of fault-location is 0.0509%.

Furthermore, branch M_1–M_{10}, line M_9–b_{12}, and line M_8–b_{11} are modified from overhead lines to cables (the percentage length of the cable is 34%), and conversion errors of 0, 5%, 10%, 15%, and 20% are considered. The fault-location percent errors of the proposed method and the errors of the aforementioned existing method are shown in Fig. 8. From this figure, the maximum and average percent errors of the proposed method are 0.0342% (i.e., 6.67 m) and 0.0284% (i.e., 5.54 m). Meanwhile, the proposed method performs better than the existing method. The maximum percent error decreases by 0.5762% (i.e., 112 m). The average percent decreases by 0.5376% (i.e., 105 m).

TABLE 8. The converted fault distances.

Original Distance (m)	Converted Distance (m)	Original Distance (m)	Converted Distance (m)	Original Distance (m)	Converted Distance (m)
2400	2318.52	2400	2318.52	2400	2318.52
2400	2318.52	2400	2318.52	2360	2295.32
2400	2318.52	2360	2295.32	2420	2330.12
2360	2295.32	2380	2306.92	2400	2318.52
2380	2306.92	2400	2318.52	2380	2306.92

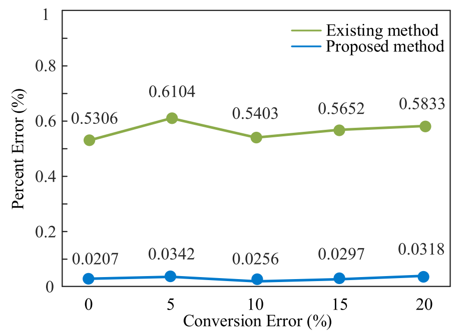

FIGURE 8. Percent errors of the proposed method and the existing method considering the conversion error.

TABLE 9. Errors of fault location under different fault conditions.

Fault location	Fault resistance (Ω)	Fault angle (°)	Fault type	Error (%)
f_2	100	10	A-g	0.0281
f_3	500	45	A-g	0.0232
f_4	1000	90	A-g	0.0201
f_5	1500	135	A-g	0.0299
f_2	5	10	AB	0.0189
f_3	10	45	AB	0.0175
f_4	15	90	AB	0.0104
f_5	20	135	AB	0.0167
f_2	5	10	AB-g	0.0202
f_3	10	45	AB-g	0.0148
f_4	15	90	AB-g	0.0136
f_5	20	135	AB-g	0.0141
f_2	5	10	ABC	0.0163
f_3	10	45	ABC	0.0152
f_4	15	90	ABC	0.0116
f_5	20	135	ABC	0.0137

E. PERFORMANCE OF THE PROPOSED METHOD UNDER DIFFERENT FAULT CONDITIONS

Here, four fault conditions are considered: fault locations, fault resistance, fault type and fault inception angle. To investigate the performance of the proposed method, various simulation cases are tested, and the fault-location errors are presented in TABLE 9. In TABLE 9, f_2, f_3, f_4, and f_5 are 568 m, 3460 m, 2830 m, and 2235 m from M*, respectively.

It can be calculated that the maximum and average errors are 0.0299% and 0.0178%, respectively. Therefore, the effect of fault conditions on the accuracy of the proposed method is not considerable.

V. CONCLUSION

This paper proposes and validates a novel CFTD-based method for fault location in branched power distribution networks. This method performs better than existing methods because it does not require the identification of the faulted branch. In the proposed method, the CFTD calculated by the first arrival times of the fault-generated traveling waves detected at each branch terminal is applied to search out the fault point. The quartile method is used to eliminate the influence of arrival time errors on the fault-location accuracy. It is shown that the proposed method provides results with high accuracy even if a large error exists in a single arrival time or nonidentical errors exist in all arrival times. Moreover, the proposed method presents a strong stability of traveling-wave velocity, which overcomes the impact of an inaccurate or unknown velocity in practice.

REFERENCES

[1] A. H. P. Cavalcante and C. M. de Almeida, "Fault location approach for distribution systems based on modern monitoring infrastructure," *IET Generat., Transmiss. Distrib.*, vol. 12, no. 1, pp. 94–103, Jan. 2018.

[2] F. Deng, X. Zeng, and L. Pan, "Research on multi-terminal traveling wave fault location method in complicated networks based on cloud computing," *Protection Control Mod. Power Syst.*, vol. 2, no. 2, pp. 2–19, 2017.

[3] M. Daisy and R. Dashti, "Single phase fault location in electrical distribution feeder using hybrid method," *Energy*, vol. 133, pp. 356–368, May 2016.

[4] L. Ji, X. Tao, Y. Fu, Y. Mi, and Z. Li, "A new single ended fault location method for transmission lime based onpositive sequence superimposed network during auto-reclosing," *IEEE Trans. Power Del.*, vol. 34, no. 3, pp. 1019–1029, Jun. 2019.

[5] R. Dashti and J. Sadeh, "Fault section estimation in power distribution network using impedance-based fault distance calculation and frequency spectrum analysis," *IET Gener., Transmiss. Distrib.*, vol. 8, no. 8, pp. 1406–1417, Aug. 2014.

[6] O. Naidu and A. K. Pradhan, "A traveling wave-based fault location method using unsynchronized current measurements," *IEEE Trans. Power Del.*, vol. 34, no. 2, pp. 505–513, Apr. 2019.

[7] Y. Xi, Z. Li, X. Zeng, X. Tang, X. Zhang, and H. Xiao, "Fault location based on traveling wave identification using an adaptive extended kalman filter," *IET Generat., Transmiss. Distrib.*, vol. 12, no. 6, pp. 1314–1322, Mar. 2018.

[8] F. V. Lopes, "Setting-free traveling-wave-based earth fault location using unsynchronized two-terminal data," *IEEE Trans. Power Del.*, vol. 31, no. 5, pp. 2296–2298, Oct. 2016.

[9] D. Tzelepis, G. Fusiek, A. Dysko, P. Niewczas, C. Booth, and X. Dong, "Novel fault location in MTDC grids with non-homogeneous transmission lines utilizing distributed current sensing technology," *IEEE Trans. Smart Grid*, vol. 9, no. 5, pp. 5432–5443, Sep. 2018.

[10] F. V. Lopes, B. F. Kusel, and K. M. Silva, "Traveling wave-based fault location on half-wavelength transmission lines," *IEEE Latin Amer. Trans.*, vol. 14, no. 1, pp. 248–253, Jan. 2016.

[11] M. U. Usman and M. O. Faruque, "Validation of a PMU-based fault location identification method for smart distribution network with photovoltaics using real-time data," *IET Gener., Transmiss. Distrib.*, vol. 12, no. 21, pp. 5824–5833, Sep. 2018.

[12] R. Dashti, M. Daisy, H. R. Shaker, and M. Tahavori, "Impedance-based fault location method for four-wire power distribution networks," *IEEE Access*, vol. 6, pp. 1342–1349, 2018.

[13] G. Manassero, S. G. D. Santo, and L. Souto, "Heuristic method for fault location in distribution feeders with the presence of distributed generation," *IEEE Smart Grid*, vol. 8, no. 6, pp. 2849–2858, Nov. 2017.

[14] S. Robson, A. Haddad, and H. Griffiths, "Fault location on branched networks using a multiended approach," *IEEE Trans. Power Del*, vol. 29, no. 4, pp. 1955–1963, Aug. 2014.

[15] A. K. Apolo and G. D. Ferreira, "Faulted branch location in distribution networks based on the analysis of high-frequency transients," *IEEE Latin Amer. Trans.*, vol. 16, no. 8, pp. 2207–2212, Aug. 2018.

[16] A. Alireza and S. M. Shahrtash, "Transient-based fault-location method for multiterminal lines employing S-transform," *IEEE Trans. Power Del.*, vol. 28, no. 3, pp. 1373–1380, Jul. 2013.

[17] M. Zahra, M. Movahhedneya, and M. Pazoki, "Gabor transform-based fault location method for multi-terminal transmission lines," *Measurement*, vol. 125, pp. 667–679, May 2018.

[18] M. Salehi and F. Namdari, "Fault location on branched networks using mathematical morphology," *IET Gener., Transmiss. Distrib.*, vol. 12, no. 1, pp. 207–216, Jan. 2018.

[19] J. Ding, X. Wang, Y. Zheng, and L. Li, "Distributed traveling-wave-based fault-location algorithm embedded in multiterminal transmission lines," *IEEE Trans. Power Del.*, vol. 33, no. 6, pp. 3045–3054, Dec. 2018.

[20] F. V. Lopes, K. M. Dantas, K. M. Silva, and F. B. Costa, "Accurate two-terminal transmission line fault location using traveling waves," *IEEE Trans. Power Del.*, vol. 33, no. 2, pp. 873–880, Apr. 2018.

[21] M. Korkali, H. Lev-Ari, and A. Abur, "Traveling-wave-based fault-location technique for transmission grids via wide-area synchronized voltage measurements," *IEEE Trans. Power Syst.*, vol. 27, no. 2, pp. 1003–1011, May 2012.

[22] C. Xi, Q. Chen, and L. Wang, "A single-terminal traveling wave fault location method for VSC-HVDC transmission lines based on S-transform," in *Proc. APPEEC*, Xi'an, China, 2016, pp. 1008–1012.

[23] M. Shafiullah and M. A. Abido, "S-transform based FFNN approach for distribution grids fault detection and classification," *IEEE Access*, vol. 6, pp. 8080–8088, 2018.

[24] F. B. Costa, B. A. Souza, and N. S. D. Brito, "Real-time detection of fault-induced transient in transmission lines," *IET Electron. Lett.*, vol. 46, pp. 753–755, May 2010.

[25] F. V. Lopes, D. Fernandes, and W. L. A. Neves, "A traveling-wave detection method based on Park's transformation for fault locators," *IEEE Trans. Power Del.*, vol. 28, no. 3, pp. 1626–1634, Jul. 2013.

[26] J. R. Hyndman and Y. Fan, "Sample quantiles in statistical packages," *Amer. Statistician*, vol. 5, no. 4, pp. 361–365, Nov. 1996.

[27] Y. Ning, D. Wang, Y. Li, and H. Zhang, "Location of faulty section and faults in hybrid multi-terminal lines based on traveling wave method," *Energies*, vol. 11, pp. 1105–1123, May 2018.

[28] Univ. Strathclyde, Glasgow, U.K. *United Kingdom Generic Distribution System.* Accessed: Dec. 2015. [Online]. Available: http//www.sedg.ac.uk/ukgds

[29] J. R. Marti, "Accurate modelling of frequency-dependent transmission lines in electromagnetic transient simulations," *IEEE Trans. Power App. Syst.*, vol. PAS-101, no. 1, pp. 147–157, Jan. 1982.

RUI CHEN was born in Ningxia, China, in 1991. He received the B.S. degree from the Wenhua College, Wuhan, China, in 2013, and the M.S. degree from the Kunming University of Science and Technology, Kunming, China, in 2016. He is currently pursuing the Ph.D. degree in power electrical engineering from the Huazhong University of Science and Technology. His research interests include fault location and protective relaying of distribution systems.

XIN YIN (M'16) received the B.Eng. degree in electronic engineering from The University of Sheffield, U.K., in 2008, the M.Sc. degree in telecommunications from University College London, U.K., in 2009, and the Ph.D. degree in electrical and electronic engineering from the University of Manchester, U.K., in 2016. He is currently a Postdoctoral Research Associate of electrical engineering with The University of Liverpool. His current research interests include distribution systems and microgrid control with renewable energy.

XIANGGEN YIN (M'08) received the B.S., M.S., and Ph.D. degrees in electrical engineering from the Huazhong University of Science and Technology (HUST), Wuhan, China, in 1982, 1985, and 1989, respectively. He is currently a Professor with the School of Electrical and Electronic Engineering, HUST. His research interests include fault location, protective relaying, and power system stability control.

YILIN LI received the B.S. degree from Central South University, Changsha, China, in 2016, and the M.S. degree from the Huazhong University of Science and Technology, Wuhan, China, in 2019. Her research interests include fault location and protection of distribution systems, and transient signal analysis.

JIAYUAN LIN received the B.S. degree from the Huazhong University of Science and Technology, Wuhan, China, in 2016, where she is currently pursuing the M.S. degree in power electrical engineering. Her research interests include fault location and distribution systems.